Paper: K^0_S and Λ Production in Jets and the Underlying Event in p–Pb at $\sqrt{s_\mathrm{NN}} = 5.02$ TeV with ALCE – Physics Results

Contents

List of Figures

1 Λ-to-K^0_S ratio in jets as a function of p_T

1.1 Λ-to-K^0_S ratio in jets with various resolution parameters

1.1.1 V0A Event Activity Estimator

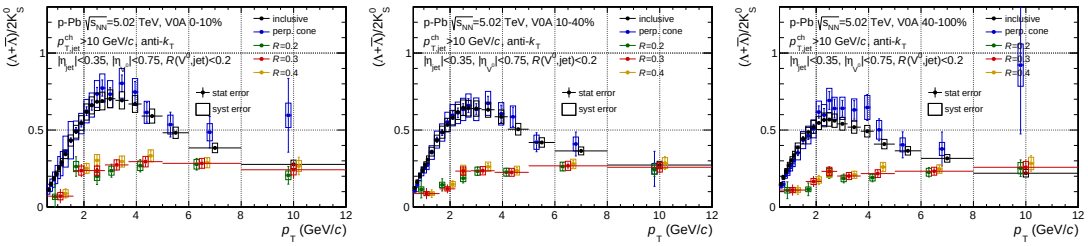

Figure 1: Λ-to-K^0_S ratio as a function of p_T obtained in jets with three different jet resolution parameters $R = 0.2,\ 0.3$ and 0.4 and, $p_{T,jet} > 10$ GeV/c. The V^0–jet matching radius $R(V^0, \text{jet}) < 0.2$. Results are shown in three V0A event activity classes and compared with the inclusive and the underlying V^0s.

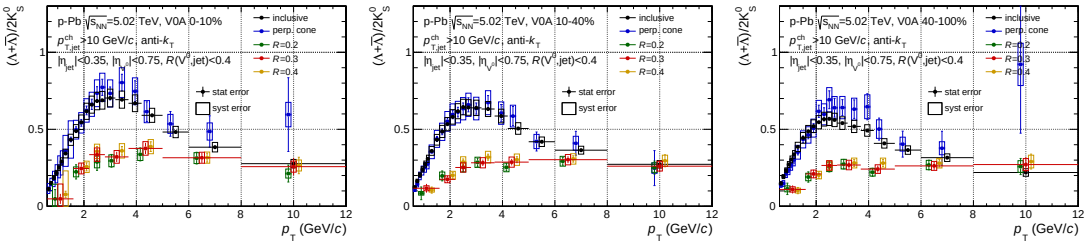

Figure 2: Λ-to-K^0_S ratio as a function of p_T obtained in jets with three different jet resolution parameters $R = 0.2,\ 0.3$ and 0.4 and, $p_{T,jet} > 10$ GeV/c. The V^0–jet matching radius $R(V^0, \text{jet}) < 0.4$. Results are shown in three V0A event activity classes and compared with the inclusive and the underlying V^0s.

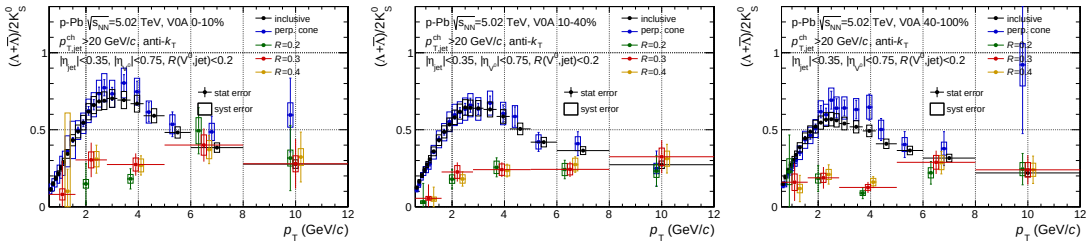

Figure 3: Λ-to-K^0_S ratio as a function of p_T obtained in jets with three different jet resolution parameters $R = 0.2,\ 0.3$ and 0.4 and, $p_{T,jet} > 20$ GeV/c. The V^0–jet matching radius $R(V^0, \text{jet}) < 0.2$. Results are shown in three V0A event activity classes and compared with the inclusive and the underlying V^0s.

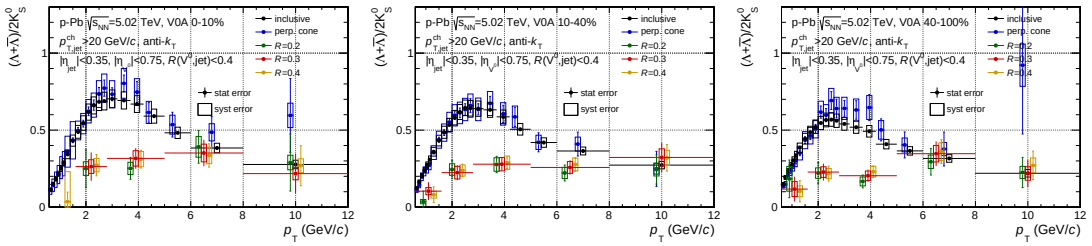

Figure 4: Λ-to-K^0_S ratio as a function of p_T obtained in jets with three different jet resolution parameters $R = 0.2,\ 0.3$ and 0.4 and, $p_{T,jet} > 20$ GeV/c. The V^0–jet matching radius $R(V^0, \text{jet}) < 0.4$. Results are shown in three V0A event activity classes and compared with the inclusive and the underlying V^0s.

1.1.2 ZNA Event Activity Estimator

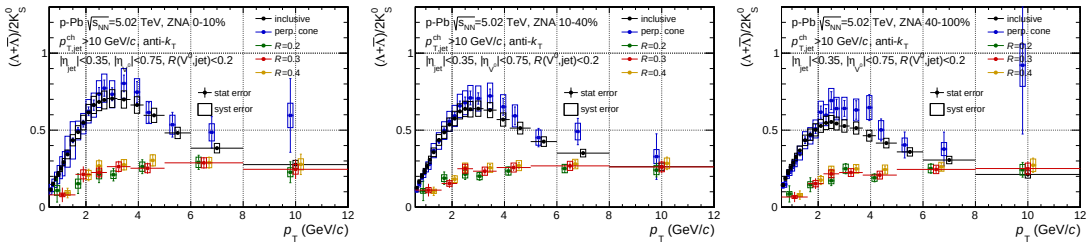

Figure 5: Λ-to-K^0_S ratio as a function of p_T obtained in jets with three different jet resolution parameters $R = 0.2,\ 0.3$ and 0.4 and, $p_{T,jet} > 10$ GeV/c. The V^0–jet matching radius $R(V^0, \text{jet}) < 0.2$. Results are shown in three ZNA event activity classes and compared with the inclusive and the underlying V^0s.

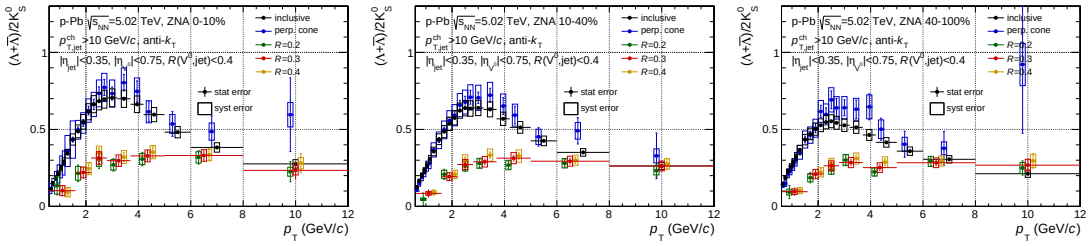

Figure 6: Λ-to-K^0_S ratio as a function of p_T obtained in jets with three different jet resolution parameters $R = 0.2,\ 0.3$ and 0.4 and, $p_{T,jet} > 10$ GeV/c. The V^0–jet matching radius $R(V^0, \text{jet}) < 0.4$. Results are shown in three ZNA event activity classes and compared with the inclusive and the underlying V^0s.

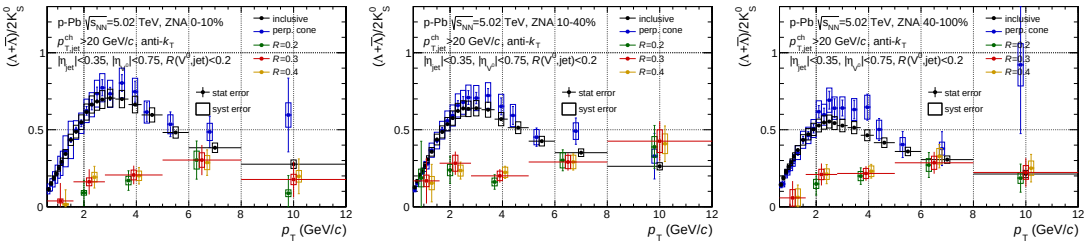

Figure 7: Λ-to-K^0_S ratio as a function of p_T obtained in jets with three different jet resolution parameters $R = 0.2,\ 0.3$ and 0.4 and, $p_{T,jet} > 20$ GeV/c. The V^0–jet matching radius $R(V^0, \text{jet}) < 0.2$. Results are shown in three ZNA event activity classes and compared with the inclusive and the underlying V^0s.

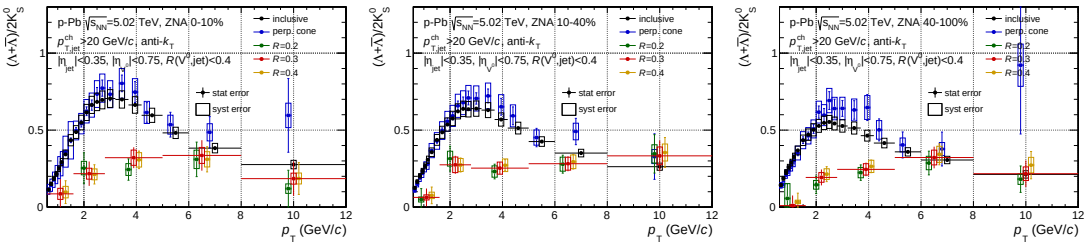

Figure 8: Λ-to-K^0_S ratio as a function of p_T obtained in jets with three different jet resolution parameters $R = 0.2,\ 0.3$ and 0.4 and, $p_{T,jet} > 20$ GeV/c. The V^0–jet matching radius $R(V^0, \text{jet}) < 0.4$. Results are shown in three ZNA event activity classes and compared with the inclusive and the underlying V^0s.

1.2 Λ-to-K^0_S ratio in jets averaged over $R = 0.2,\ 0.3$ and 0.4

1.2.1 V0A Event Activity Estimator

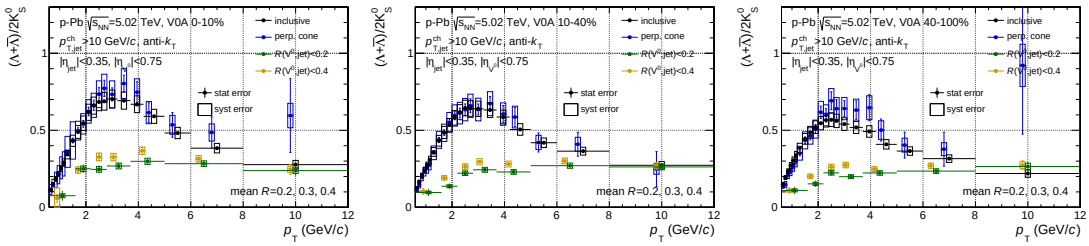

Figure 9: Λ-to-K^0_S ratio as a function of p_T averaged over jets with $R = 0.2,\ 0.3$ and 0.4 in $p_{T,jet} > 10$ GeV/c. Two V^0–jet matching radii $R(V^0, jet) < 0.2$ and 0.4 are used. Results are shown in three V0A event activity classes and compared with the inclusive and the underlying V^0s.

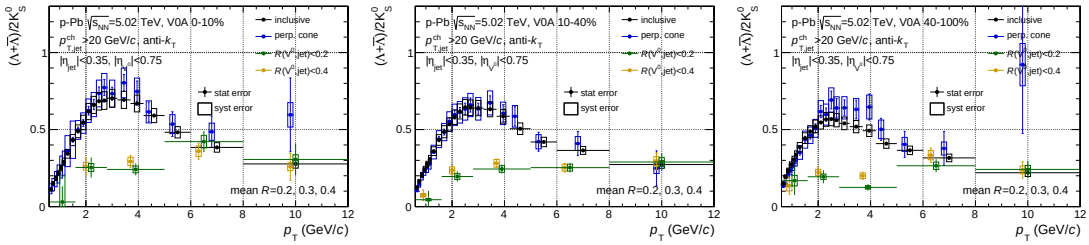

Figure 10: Λ-to-K^0_S ratio as a function of p_T averaged over jets with $R = 0.2,\ 0.3$ and 0.4 in $p_{T,jet} > 20$ GeV/c. Two V^0–jet matching radii $R(V^0, jet) < 0.2$ and 0.4 are used. Results are shown in three V0A event activity classes and compared with the inclusive and the underlying V^0s.

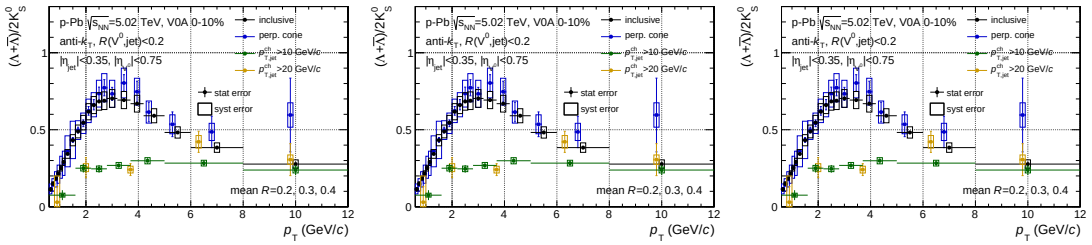

Figure 11: Λ-to-K^0_S ratio as a function of p_T averaged over jets with $R = 0.2,\ 0.3$ and 0.4 in $p_{T,jet} > 10$ and > 20 GeV/c, respectively. V^0–jet matching radius $R(V^0, \text{jet}) < 0.2$. Results are shown in three V0A event activity classes and compared with the inclusive and the underlying V^0s.

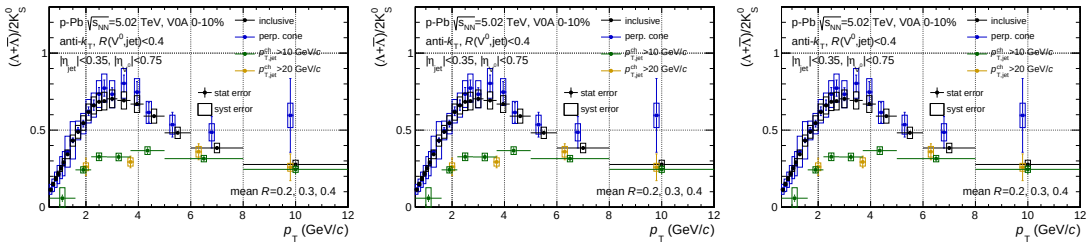

Figure 12: Λ-to-K^0_S ratio as a function of p_T averaged over jets with $R = 0.2,\ 0.3$ and 0.4 in $p_{T,jet} > 10$ and > 20 GeV/c, respectively. V^0–jet matching radius $R(V^0, \text{jet}) < 0.4$. Results are shown in three V0A event activity classes and compared with the inclusive and the underlying V^0s.

1.2.2 ZNA Event Activity Estimator

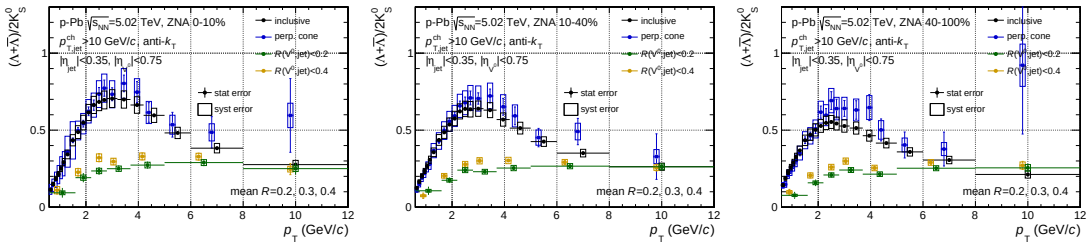

Figure 13: Λ-to-K^0_S ratio as a function of p_T averaged over jets with $R = 0.2,\ 0.3$ and 0.4 in $p_{T,jet} > 10$ GeV/c. Two V^0–jet matching radii $R(V^0, jet) < 0.2$ and 0.4 are used. Results are shown in three ZNA event activity classes and compared with the inclusive and the underlying V^0s.

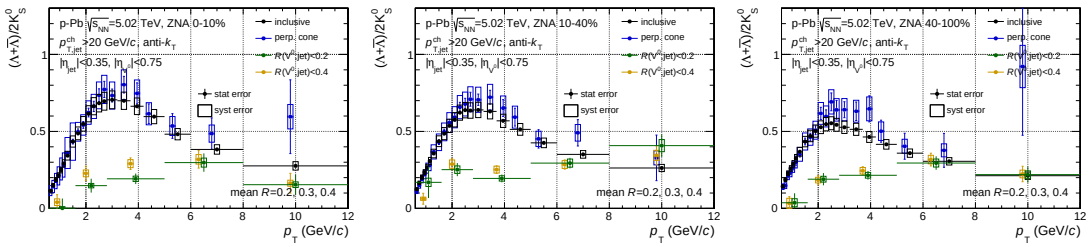

Figure 14: Λ-to-K^0_S ratio as a function of p_T averaged over jets with $R = 0.2,\ 0.3$ and 0.4 in $p_{T,jet} > 20$ GeV/c. Two V^0–jet matching radii $R(V^0, jet) < 0.2$ and 0.4 are used. Results are shown in three ZNA event activity classes and compared with the inclusive and the underlying V^0s.

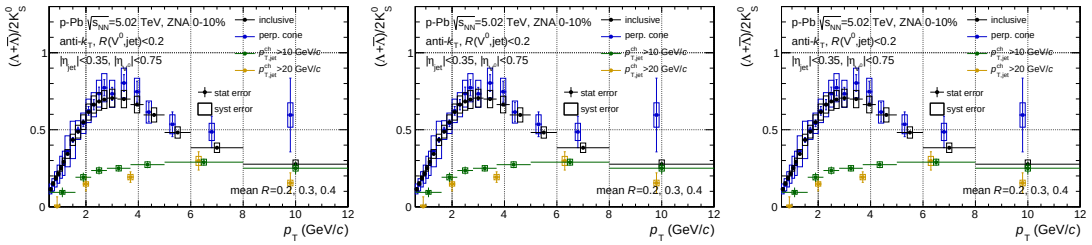

Figure 15: Λ-to-K^0_S ratio as a function of p_T averaged over jets with $R = 0.2,\ 0.3$ and 0.4 in $p_{T,jet} > 10$ and > 20 GeV/c, respectively. V^0–jet matching radius $R(V^0, \text{jet}) < 0.2$. Results are shown in three ZNA event activity classes and compared with the inclusive and the underlying V^0s.

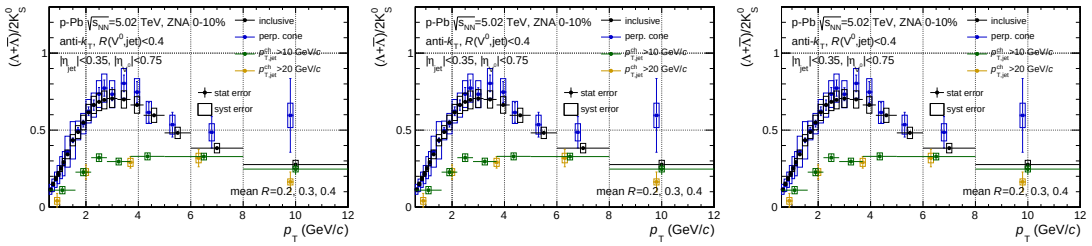

Figure 16: Λ-to-K^0_S ratio as a function of p_T averaged over jets with $R = 0.2,\ 0.3$ and 0.4 in $p_{T,jet} > 10$ and > 20 GeV/c, respectively. V^0–jet matching radius $R(V^0, \text{jet}) < 0.4$. Results are shown in three ZNA event activity classes and compared with the inclusive and the underlying V^0s.

2 Λ-to-K^0_S ratio as a function of matching radius

2.1 V^0 density as a function of matching radius

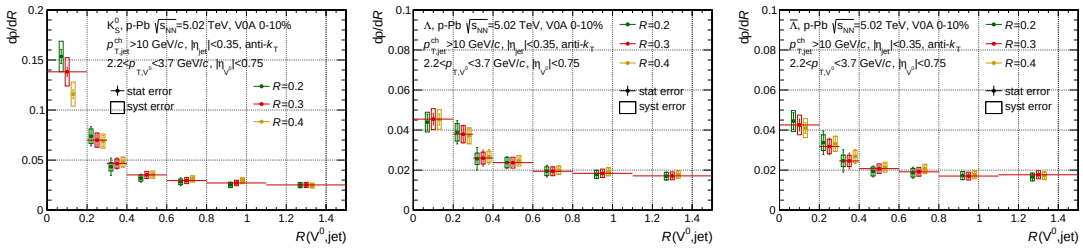

Figure 17: V^0 density spectra as a function of matching radius $R(V^0, \text{jet})$ in jets with resolution parameters $R = 0.2,\ 0.3$ and 0.4 and in $p_{T,\text{jet}} > 10$ GeV/c. V^0s are obtained in $2.2 < p_T < 3.7$ GeV/c. Results are shown in $0 - 10\%$ V0A event activity class. The underlying V^0s are not subtracted.

2.2 Λ-to-K^0_S ratio average over jets resolution parameters

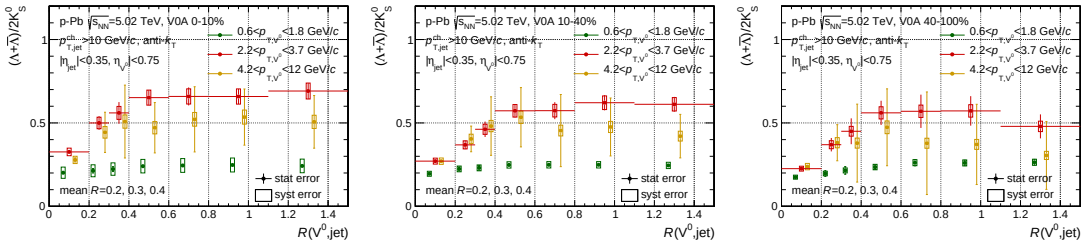

Figure 18: Λ-to-K^0_S ratio as a function of matching radius $R(V^0, \text{jet})$ in jets averaged over resolution parameters $R = 0.2,\ 0.3$ and 0.4 and in $p_{T,\text{jet}} > 10$ GeV/c. Results are shown in three V^0 p_T regions and three V0A event activity classes. The underlying V^0s are not subtracted.

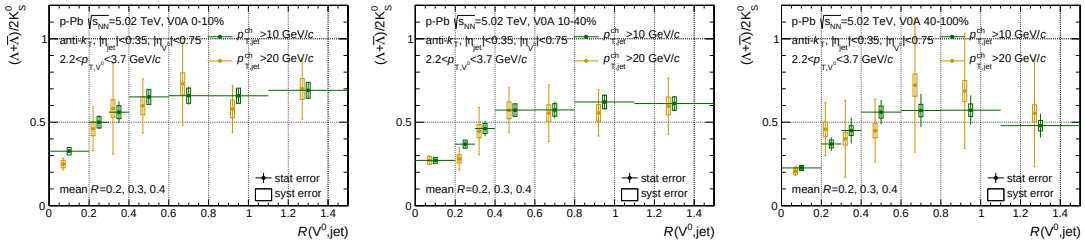

Figure 19: Λ-to-K^0_S ratio as a function of matching radius $R(V^0, \text{jet})$ in jets averaged over resolution parameters $R = 0.2,\ 0.3$ and 0.4 and in $p_{T,\text{jet}} > 10$ and 20 GeV/c, respectively. Results are shown in $2.2 < p_T < 3.7$ GeV/c and three V0A event activity classes. The underlying V^0s are not subtracted.

3 Mean p_{T} of V^0s

3.1 V^0 mean p_{T} as a function of event multiplicity

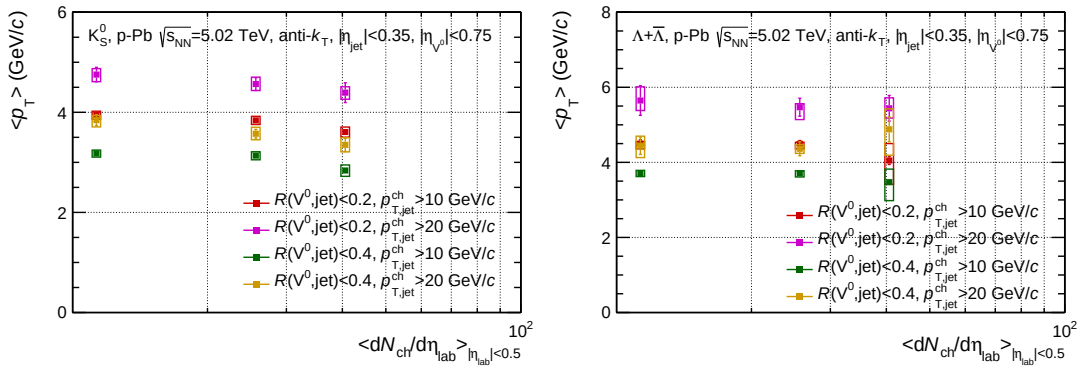

Figure 20: Mean p_{T} of V^0s in jets averaged over resolution parameter $R = 0.2,\ 0.3$ and 0.4 in varius matching radii and jet p_{T} regions.

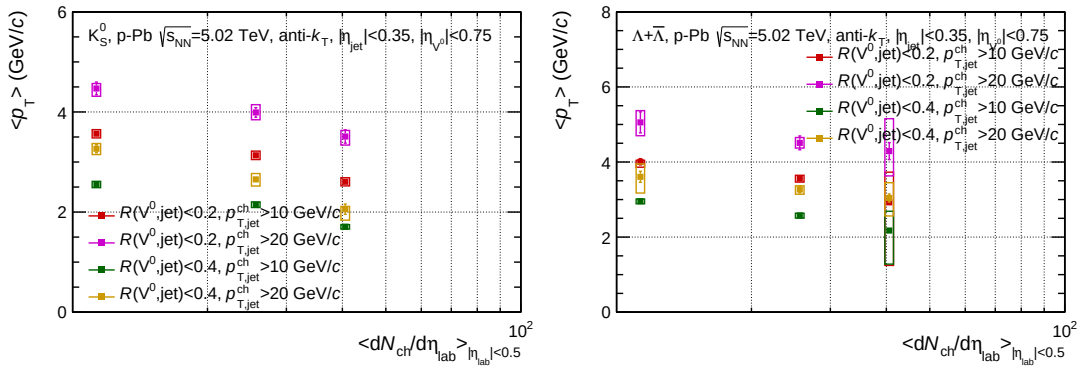

Figure 21: Mean p_{T} of V^0s in jets averaged over resolution parameter $R = 0.2,\ 0.3$ and 0.4 in varius matching radii and jet p_{T} regions. The underlying V^0s are not subtracted.

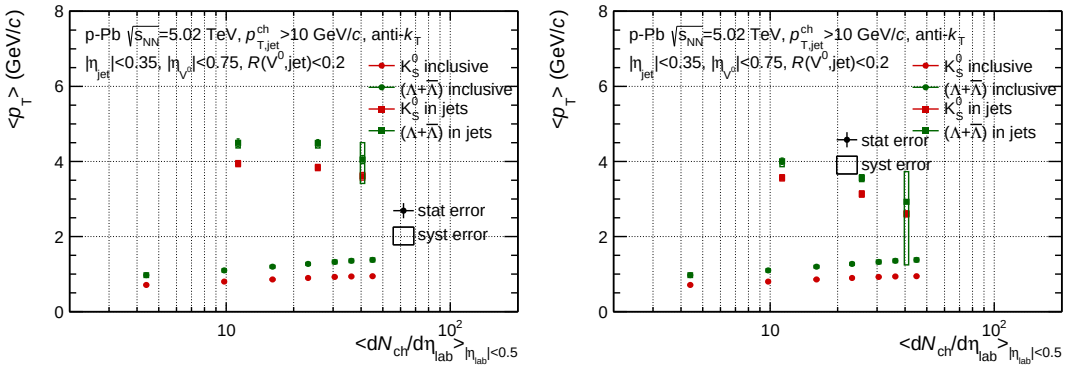

Figure 22: Mean p_{T} of V^0s in jets averaged over resolution parameter $R = 0.2,\ 0.3$ and 0.4 with V^0–jet matching radius $R(\mathrm{V}^0, \mathrm{jet}) < 0.2$ and in $p_{\mathrm{T,jet}} > 10$ GeV/c. The results with and without the underlying V^0 subtraction are shown in high and left, respectively.

3.2 V^0 mean p_{T} as a function of matching radius

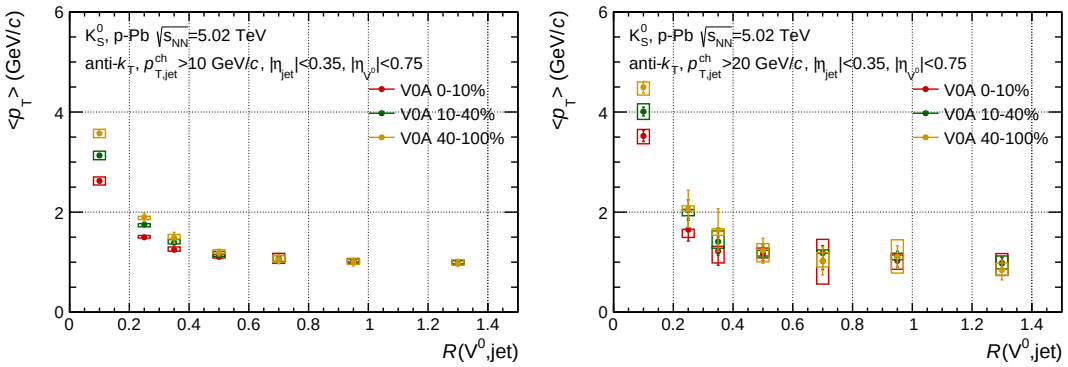

Figure 23: Mean p_{T} of $\mathrm{K}^0_{\mathrm{S}}$ as a function of matched radius in jets averaged over resolution parameter $R = 0.2,\ 0.3$ and 0.4 in $p_{\mathrm{T,jet}} > 10$ and 20 GeV/c. The underlying V^0s are not subtracted.

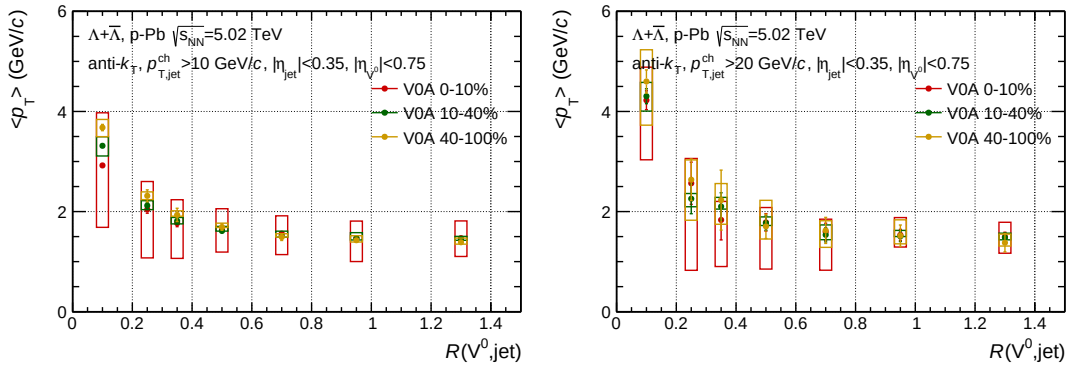

Figure 24: Mean p_{T} of $\Lambda + \overline{\Lambda}$ as a function of matched radius in jets averaged over resolution parameter $R = 0.2,\ 0.3$ and 0.4 in $p_{\mathrm{T,jet}} > 10$ and 20 GeV/c. The underlying V^0s are not subtracted.

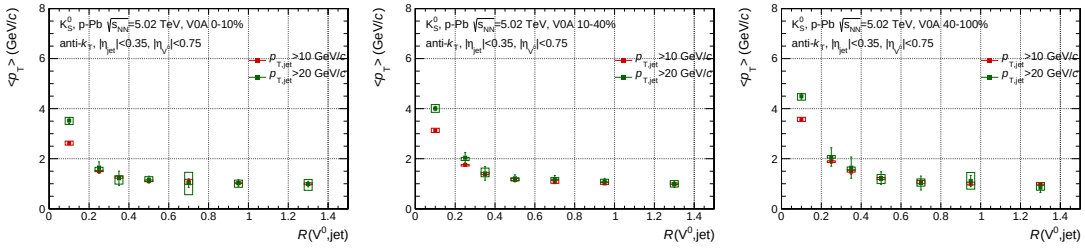

Figure 25: Mean p_{T} and $\mathrm{K}^0_{\mathrm{S}}$ as a function of matched radius in jets averaged over resolution parameter $R = 0.2,\ 0.3$ and 0.4 in $p_{\mathrm{T,jet}} > 10$ GeV/c and 20 GeV/c. Results are shown in three V0A event activity classes. The underlying V^0s are not subtracted.

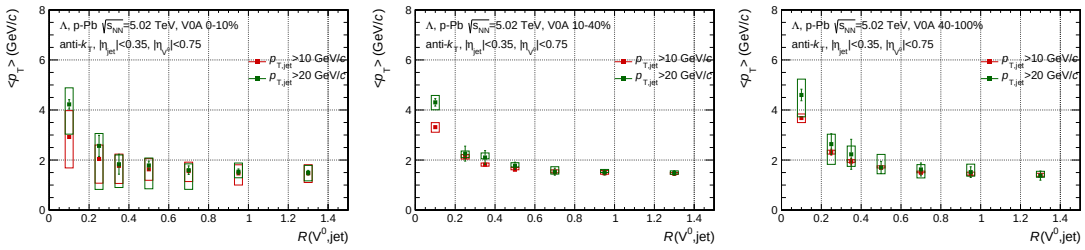

Figure 26: Mean p_{T} of $\Lambda + \overline{\Lambda}$ as a function of matched radius in jets averaged over resolution parameter $R = 0.2,\ 0.3$ and 0.4 in $p_{\mathrm{T,jet}} > 10$ and 20 GeV/c. Results are shown in three V0A event activity classes. The underlying V^0s are not subtracted.

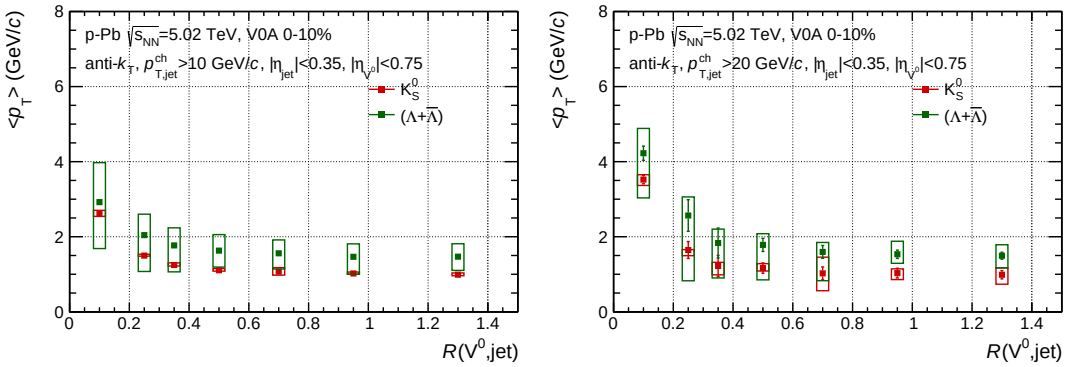

Figure 27: Mean p_{T} of V^0s as a function of matched radius in jets averaged over resolution parameter $R = 0.2,\ 0.3$ and 0.4 in $p_{\mathrm{T,jet}} > 10$ GeV/c. The underlying V^0s are not subtracted.

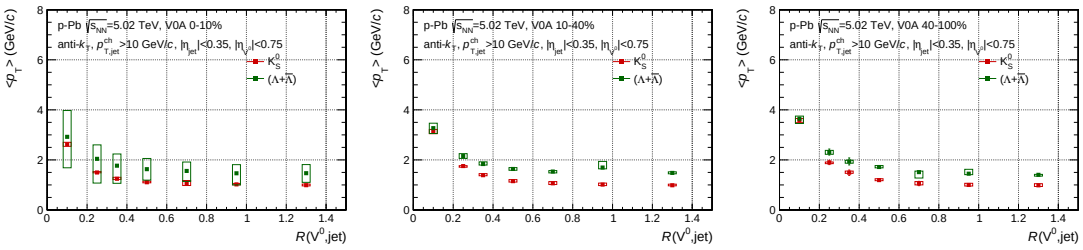

Figure 28: Mean p_{T} of V^0s as a function of matched radius in jets averaged over resolution parameter $R = 0.2,\ 0.3$ and 0.4 in $p_{\mathrm{T,jet}} > 10$ GeV/c. Results are shown in three V0A event activity classes. The underlying V^0s are not subtracted.